original article

Diabetes, Obesity and Metabolism 13: 337–347, 2011.

ORIGINAL ARTICLE

Effects of chronic administration of alogliptin on the development of diabetes and β-cell function in high fat diet/streptozotocin diabetic mice

X. Zhang, Z. Wang, Y. Huang & J. Wang

Department of Pharmaceutical Sciences, College of Pharmacy, Western University of Health Sciences, Pomona, CA, USA

Aim: Alogliptin is a potent and highly selective dipeptidyl peptidase-4 (DPP-4) inhibitor. The aim of this study was to determine its effects on glucose control and pancreas islet function and to identify the underlying molecular mechanisms after chronic administration, in a non-genetic mouse model of type 2 diabetes.

Methods: Alogliptin (5, 15 and 45 mg/kg) was orally administered to high fat diet/streptozotocin (HFD/STZ) diabetic mice daily for 10 weeks. Postprandial and 6-h fasting blood glucose levels, blood A1C level, oral glucose tolerance and pancreas insulin content were measured during or after the treatment period. Alogliptin plasma concentration was determined by an LC/MS/MS method. Islet morphology and architectural changes were evaluated with immunohistochemical analysis. Islet endocrine secretion ability was assessed by measuring insulin release from isolated islets which were challenged with 16 mM glucose and 30 mM potassium chloride, respectively. Gene expression profiles of the pancreas were analysed using the mouse diabetes RT^2 Profiler PCR array which contains 84 genes related to the onset, development and progression of diabetes.

Results: Alogliptin showed dose-dependent reduction of postprandial and fasting blood glucose levels and blood A1C levels. Glucose clearance ability and pancreas insulin content were both increased. Alogliptin significantly restored the β-cell mass and islet morphology, thus preserving islet function of insulin secretion. Expression of 10 genes including *Ins1* was significantly changed in the pancreas of diabetic mice. Chronic alogliptin treatment completely or partially reversed the abnormalities in gene expression.

Conclusions: Chronic treatment of alogliptin improved glucose control and facilitated restoration of islet architecture and function in HFD/STZ diabetic mice. The gene expression profiles suggest that the underlying molecular mechanisms of β-cell protection by alogliptin may involve alleviating endoplasmic reticulum burden and mitochondria oxidative stress, increasing β-cell differentiation and proliferation, enhancing islet architecture remodelling and preserving islet function.

Keywords: alogliptin, antidiabetic drug, β-cells, DPP-IV inhibitor, glycaemic control, islets, type 2 diabetes, type 2 diabetes mellitus

Date submitted 1 September 2010; date of first decision 1 October 2010; date of final acceptance 3 December 2010

Introduction

Type 2 diabetes mellitus (T2DM) is considered as a chronic metabolic disease because of insulin resistance and β-cell dysfunction. It is characterized by impaired insulin responsiveness and anatomical abnormalities of the pancreatic islets during the course of the disease [1,2]. Most conventional antidiabetic drugs, including sulphonylureas and thiazolidinediones, focus on improving glucose control and thus protecting pancreas from glucotoxicity and lipotoxicity during the initial process of treatment. However, the loss of glucose control may be further deteriorated over the years and therefore most T2DM patients eventually need additional insulin supplement for disease control [3]. As the mechanism of insulin resistance is still unclear [4–6], treatment of T2DM becomes complex and the therapeutic goal is difficult to achieve [7]. Thus, there has been little improvement on the management of the metabolic syndrome and the control of the prevalence of T2DM [8]. New therapies with islet protection and β-cell function improvement are needed to prevent or delay the onset of the disease and to modify its pathologic development after the onset [9].

Currently, only incretins and their analogues are considered as insulinotropic agents that can improve β-cell function [10]. Two known incretin hormones, glucose-dependent insulinotropic polypeptide (GIP) and glucagon-like peptide-1 (GLP-1), are gut-derived peptides secreted, respectively, from the K- and L-cell of intestinal epithelia in response to nutrient ingestion. They act through structurally distinct yet related incretin receptors on β-cells to increase glucose-dependent insulin secretion, β-cell proliferation and resistance to apoptosis [11–13]. Their functions are divided into those mediating primarily acute responses, such as potentiation of insulin secretion, and those mediating chronic responses, such as gene transcriptional changes and cell replication [14]. Clinical applications of GLP-1 or its analogues such as exendin-4

Correspondence to: Dr. Jeffrey Wang, Department of Pharmaceutical Sciences, College of Pharmacy, Western University of Health Sciences, 309 E. Second Street, Pomona, CA 91766, USA.
E-mail: jwang@westernu.edu

have shown remarkable glucose-lowering effect with increased β-cell volume and insulin secretion in diabetic subjects [15]. The direct insulinotropic effects of these agents on β-cell make possible a promising way for β-cell preservation [16]. However, GLP-1 and GIP are rapidly degraded and inactivated *in vivo*, primarily by the enzyme dipeptidyl peptidase-4 (DPP-4) [17]. In T2DM patients, the incretin effects were found to be impaired [18]. Therefore, developing DPP-4 inhibitors to prolong the effects of endogenous incretins became a logic strategy [19].

Alogliptin (SYR-322, 2-[6-[(3*R*)-3-amino-1-piperidinyl]-3,4-dihydro-3-methyl-2,4-dioxo-1(2*H*) pyrimidinyl]methyl] benzonitrile monobenzoate) is a quinazolinone-based DPP-4 inhibitor, being developed for once-daily oral dosing to improve glucose control in T2DM patients [20]. Alogliptin is potent (IC_{50} < 10 nM) and >10 000-fold more selective for targeting DPP-4 than other related serine proteases including DPP-2, DPP-8 and DPP-9 [20,21]. In Wistar fatty rats and neonatal streptozotocin-treated diabetic NSTZ-1.5 rats (an obese and a non-obese rat model of T2DM, respectively [22,23]), a single dose of alogliptin improved glucose tolerance and increased early-phase insulin secretion following an oral glucose challenge. In another experiment with NSTZ-1.5 rats, chronic treatment with alogliptin for 4 weeks decreased glycosylated haemoglobin (A1C) level and increased pancreatic insulin content [24]. In addition, alogliptin dose-dependently improved glucose control, decreased triglyceride level and improved β-cell function in *ob/ob* mice, correlating with the inhibition of blood DPP-4 activity and increased GLP-1 level [25].

In this study, we characterized the effects of chronic alogliptin administration on glucose control and pancreas islet protection in a non-genetic high fat diet (HFD)/STZ mouse model for T2DM [26–29]. This model mimics the natural initiation and development of T2DM by inducing mouse obesity with HFD and partial pancreas islet damage with a low dose STZ. By comparing the gene expression profiles of different treatment groups with the control groups, we have identified the putative molecular mechanisms for the protective effects of alogliptin on the mouse pancreas.

Materials and Methods

Test Materials

Alogliptin benzoate was provided by Takeda Pharmaceuticals North America (Deerfield, IL, USA). Other reagents were purchased from Sigma-Aldrich (St. Louis, MO, USA), unless otherwise indicated.

Experimental HFD/STZ Diabetic Mice and Drug Treatment

Four-week-old male ICR mice were purchased from Taconic Farm (Germantown, NY, USA) and fed with the HFD D12492 (Research Diets, New Brunswick, NJ, USA). After 3 weeks of HFD feeding, a single low dose STZ (90 mg/kg ip, formulated in 0.1 M citrate buffer, pH 4.5) was given after a 6-h fasting to induce diabetes. Two weeks after STZ injection, 6-h fasting blood glucose level of the HFD/STZ mice was measured to confirm hyperglycaemia. Mice with similar degree of hyperglycaemia were randomly divided into four groups: the vehicle, low dose, medium dose and high dose groups (n = 16). The vehicle group received 0.5% methylcellulose only, whereas the low dose, medium dose and high dose groups were given alogliptin at 5, 15 and 45 mg/kg in 0.5% methylcellulose, respectively. Alogliptin was dosed once daily using a gastric gavage. A normal, non-diabetic control group was included and fed with regular Teklad 8604 rodent diet (Harlan Laboratories, Indianapolis, IN, USA). All animals were housed in an environmentally controlled room at 25 °C in a 12-h light/dark cycle and given free access to food and water throughout the experimental period. Fasting animals were allowed free access to water. All animal procedures were performed using a protocol approved by the Institutional Animal Care and Use Committee of the Western University of Health Sciences.

Food Intake, Body Weight, Blood A1C Level, Postprandial and Fasting Blood Glucose Levels

Food intake and body weight were monitored weekly. Postprandial blood glucose level was determined weekly (at 09:00 hours, 3 h after the dark period) using a OneTouch Ultra 2 glucometer (LifeScan, Milpitas, CA, USA) with blood from tail bleed. The 6-h fasting glucose level was measured (at 15:00 hours, after fasting for 6 h) at weeks 0, 2, 5 and 10. Blood A1C level was measured with an A1CNow$^+$ Test kit (Bayer HealthCare, Sunnyvale, CA, USA) at weeks 0, 5 and 10.

Oral Glucose Tolerance Test

Oral glucose tolerance test was conducted at week 8. Mice were fasted for 4 h before an oral glucose load (2 g/kg). Blood samples were collected from the tail before and 15, 30, 60 and 120 min after glucose loading. Blood glucose level was determined with a OneTouch Ultra 2 glucometer (LifeScan).

Pancreatic Insulin Content

At the end of the 10-week treatment, mice were sacrificed after a 4-h fasting. The pancreas was dissected immediately and frozen at −20 °C until analysis. For the extraction of pancreatic insulin, pancreatic tissue was first incubated in acidic ethanol (1.5% HCl in 70% EtOH) at 4 °C overnight and then homogenized on ice. After another incubation at 4 °C overnight, the mixture was centrifuged and the supernatant was collected and stored at −20 °C until analysis. Insulin concentration was determined using a mouse insulin enzyme-linked immunosorbent assay (ELISA) kit (ALPCO Diagnostics, Salem, NH, USA) according to the manufacturer's instruction.

Plasma Drug Trough Concentration

At 24 h following the last dose, mice were sacrificed and blood samples were collected. The plasma samples were separated after centrifugation and kept at −80 °C until analysis. Plasma concentration of alogliptin was determined using a validated LC/MS/MS method. Briefly, 100 µl of plasma sample

were mixed with 10 µl of 1 µg/ml tramadol (the internal standard) and 10 µl of 50% methanol. The sample mixture was then combined with 200 µl acetonitrile to precipitate protein components. After centrifuged at 18 000 g for 10 min, 10 µl of the supernatant was injected into the LC/MS/MS system for analysis. A standard curve was constructed for quantification.

Assessment of Islet Endocrine Secretion Function

To assess the insulin secretion ability of islets to various secretagogues, glucose-stimulated insulin secretion (GSIS) and KCl-induced maximum insulin secretion capacity were measured by static incubation of isolated islets with glucose and KCl, respectively. Pancreatic islets were isolated using a modified method of Lacy and Kostianovsky [30] and Korbutt et al. [31]. Briefly, mouse pancreas was first torn apart into small pieces in HBSS on ice. Digestion was then performed in a water bath at 37 °C for 15 min with 0.3 mg/ml collagenase (Sigma). Islet separation was achieved by centrifugation (530 g, 15 min) on discontinuous Histopaque gradients (Histopaque 1.119, 1.083 and 1.077 g/ml; Sigma). Islets were harvested from the interface between the 1.083 and 1.077 layers. To ensure quality of the preparation, islets were further handpicked and counted under a Leica Stereozoom 4 microscope (Leica Microsystem, Wetzlar, Germany). The islets were seeded in 24-well culture plates in RPMI-1640 medium supplemented with 10% fetal calf serum, at 37 °C in a humidified incubator with 5% CO_2. Five islets were first incubated for 1 h in 1 ml RPMI-1640 medium containing 2 mM glucose. The supernatant was collected and stored at −20 °C for the analysis of basal insulin level. Islets were then challenged with 1 ml 16 mM glucose or 30 mM KCl for 1 h at 37 °C. Medium samples were collected and stored at −20 °C for the analysis of GSIS or KCl-induced maximum insulin secretion.

Histological and Immunohistochemical Analyses

Pancreas were fixed in 10% buffered formaldehyde with Zn^{2+} at 4 °C overnight and then embedded in paraffin. Serial sections were cut into a thickness of 5 µm and stained with haematoxylin and eosin (H&E) for light microscopic examination. For quantification of β- and α-cell mass ratio in each islet, tissue sections were treated with anti-insulin and antiglucagon antibodies (Invitrogen, Carlsbad, CA, USA) with 1 : 500 dilutions. Fluorescent images were taken with a Nikon DXM 1200F Hi-QE colour CCD camera attached to a Nikon fluorescent microscope (Nikon, Melville, NY, USA). The area of positive-stained β- and α-cells in each representative section was measured with a MetaVue image processing software (Molecular Devices, Downington, PA, USA). Ten randomly chosen islets from each section were used for area counting. The analysis was blindly scored by two observers. Results are expressed as mean percentage of positively stained areas within an islet.

RNA Preparation

Pancreas tissue was taken out from freshly sacrificed mouse and immersed in the RNAlater RNA stabilization reagent (Qiagen, Valencia, CA, USA) and stored at 4 °C overnight. Tissue was then homogenized and stored in Trizol reagent (Invitrogen) at −80 °C until RNA isolation. Total RNA was extracted from each sample with the RNeasy mini kit (Qiagen) according to the manufacturer's instruction. DNase I treatment was performed on each RNA sample to avoid contamination of genomic DNA. The quantity and quality of RNA were determined by measuring the UV absorbance at 260 and 280 nm with a NanoVue Plus Spectrophotometer (GE Healthcare, Piscataway, NJ, USA).

Quantitative RT-PCR Analysis Using Mouse Diabetes RT^2 Profiler PCR Arrays

RT-PCR for 84 mouse diabetes-related genes was carried out using a GeneAmp 7300 sequence detection system (Applied Biosystems, Forster City, CA, USA) with a mouse diabetes RT^2 Profile PCR array (SABiosciences, Frederick, MD, USA). Total RNA (500 ng) was used as template to synthesize cDNA with the RT^2 First Strand kit (SABiosciences). The PCR cycle condition was as follows: 94 °C for 4 min, followed by 40 cycles of 94 °C for 30 s, 62 °C for 30 s, 72 °C for 35 s and then 72 °C for 10 min. At the end of PCR cycling steps, data for each sample were displayed as a melting curve. The ABI SDS software (Applied Biosystems) was used to determine a critical threshold (Ct), which was the cycle number where the linear phase for each sample crossed the threshold level.

Gene Expression Data Analysis

After performing a precise quantification of the mRNA levels in mouse pancreas samples, the Ct values were collected using a spreadsheet template provided by SABiosciences. Data normalization was performed with the 'comparative Ct method' using a reference gene, *GAPDH*, to control experimental variation introduced by the multistage RNA processing. An average Ct was calculated and normalized to the reference gene using the following Eqn (1):

$$\Delta Ct = X - \text{Ref } (X\text{: Ct for given sample; Ref: Ct for reference sample}) \quad (1)$$

The normalized Ct was compared with the 'standard sample' using Eqn (2).

$$\Delta\Delta Ct = \Delta Ct_{sample} - \Delta Ct_{standard} \quad (2)$$

Finally, the fold change (FC) of the target gene was calculated using Eqn (3).

$$FC = 2^{-\Delta\Delta Ct} \quad \text{when} \quad \Delta\Delta Ct < 0$$
$$FC = -2^{\Delta\Delta Ct} \quad \text{when} \quad \Delta\Delta Ct > 0 \quad (3)$$

An FC > 1.5 or <−1.5 (i.e. percentage increase/decrease >50%) was considered as significant difference of gene expression.

Statistical Analysis

Data are expressed as means ± standard error. Significance of differences between two groups was determined using Student's

t-test. Significance of differences among multiple groups was assessed using one-way analysis of variance (ANOVA). A value of $p < 0.05$ was considered to be of statistic significance. Statistical and data analysis were conducted using PRISM 5.0 software package (GraphPad Software, La Jolla, CA, USA).

Results

Effect of Chronic Alogliptin Administration on Metabolic Control of HFD/STZ Mice

As shown in figure 1A, postprandial blood glucose levels in HFD/STZ mice were significantly higher than normal mice with an average value of 428 mg/dl at week 0. Over time, alogliptin significantly reduced postprandial hyperglycaemia in a dose-dependent manner. The average blood glucose levels of three alogliptin-treated groups were 80, 77 and 68% of the level of vehicle-treated group, respectively, at week 10. Similarly, 6-h fasting blood glucose levels were also dose-dependently reduced. The high dose treatment showed statistically significant decrease of glucose levels at weeks 5 and 10; whereas the medium dose reduced glucose level significantly at the end of study (figure 1B). The reduction of blood A1C levels was dose dependent and statically significant in all dose groups at weeks 5 and 10, showing an unambiguous improvement of overall glucose control by chronic alogliptin treatment (figure 1C). It is remarkable to note that the A1C value of the high dose group at week 10 was very close to that of the normal control.

The body weight and food intake were not significantly different between vehicle- and alogliptin-treated groups (data not shown). In the oral glucose tolerance test, the average blood glucose level in vehicle-treated diabetic mice was 569.0 ± 12.8 mg/dl 30 min after an oral glucose load of 2 g/kg, while that of the normal group was 237.7 ± 15.2 mg/dl (figure 1D). Alogliptin significantly reduced glucose level in all dose groups at all time points. The glucose area under the curve (AUC) of diabetic mice treated with alogliptin decreased significantly and dose dependently, suggesting the restoration of glucose excursion (figure 1D). Overall, these results showed that alogliptin exhibited glucose control in HFD/STZ diabetic mice.

Plasma Alogliptin Trough Concentration

The plasma trough concentrations of alogliptin were measured in all groups 24 h after the last oral dose. The mean plasma trough drug concentrations were 13.8 ± 5.1, 26.1 ± 7.2 and 121.4 ± 55.1 ng/ml for the low, medium and high dose groups, respectively.

Effects of Alogliptin on Islet Morphology and Architecture

After the end of the 10-week treatment, islets from non-diabetic mice showed large islets with insulin-positive β-cells (green) in the core and glucagon-positive α-cells (red) in the peripheral, with a β-cell-to-islet area ratio of 0.73 ± 0.02 (figures 2 and 3A). Vehicle-treated diabetic mice showed smaller islets with a significantly reduced β-cell-to-islet area ratio of 0.29 ± 0.08 ($p < 0.05$). There are many more glucagon-positive α-cells spotted on the surface and the core of these islets (figures 2 and 3A). The α-cell-to-islet area ratio was increased from 0.10 ± 0.01 in non-diabetic mice to 0.22 ± 0.03 in diabetic mice treated with vehicle ($p < 0.05$) (figure 3B). Alogliptin partially restored pancreatic β-cell mass and showed an intermediate morphology. Islets from the medium and high dose groups were much larger than those from the vehicle group and had significantly increased β-cell-to-islet area ratio of 0.54 ± 0.23 and 0.59 ± 0.22, respectively (figures 2 and 3A). The ratio of α-cells-to-islet area was also dose dependently reduced after alogliptin treatment, although there was no statistical significance (figure 3B). The data revealed that chronic alogliptin treatment could partially reverse the deleterious loss of β-cell mass in HFD/STZ diabetic mice and preserve the normal architecture of pancreas islets.

Pancreas Insulin Content and Islet Function

Pancreas insulin content of vehicle-treated diabetic mice was only 12% of that in non-diabetic mice at the end of the study (figure 4A). Treatment with low and medium dose alogliptin similarly led to a modest increase in islet insulin content. However, at the high dose, alogliptin significantly increased insulin content by fourfold to about 50% of that of the normal mice.

Islets from vehicle-treated diabetic mice displayed a significantly impaired response to the 16 mM glucose challenge and maximum insulin secretion induced by 30 mM KCl, in comparison to islets from normal mice (figure 4B, C). Islets from all alogliptin-treated mice exhibited significant improvement of GSIS by three- to fourfold. Maximum insulin secretion increased more than sixfold in high dose-treated mouse islets; whereas more than fivefold increases were achieved in islets from low and medium dose-treated mice.

These results indicated that chronic treatment with alogliptin significantly improved islet insulin production and secretion, which was consistent with the results that alogliptin helped recover the morphology and architecture of islets and improved blood glucose control in HFD/STZ mice.

Pancreatic Gene Expression Analysis

Expression of 10 genes among 84 tested was significantly changed between the normal group and the vehicle group (Table 1, figure 5, Table S1). Among them, seven were upregulated and three downregulated in diabetic pancreas. According to the expression products of these genes, they can be classified into five functional groups: transporters or channels (*Icam1* and *Aqp2*), metabolic enzymes (*Pfkfb3* and *G6pc*), secreted factors (*Ins1, Tgbfb1* and *Agt*), transcription factors (*Foxp3* and *Neurod1*) and mitochondrial uncoupling protein (*Ucp2*).

Pfkfb3, Agt and *Tgfb1* were upregulated by 1.73-, 1.93- and 1.59-fold, respectively. After alogliptin treatment, their expression levels were back to normal in all three dose groups. Alogliptin reversed *Agt* upregulation in a dose-dependent manner (FCs of 1.50-, 1.37- and 1.20-fold for low, medium

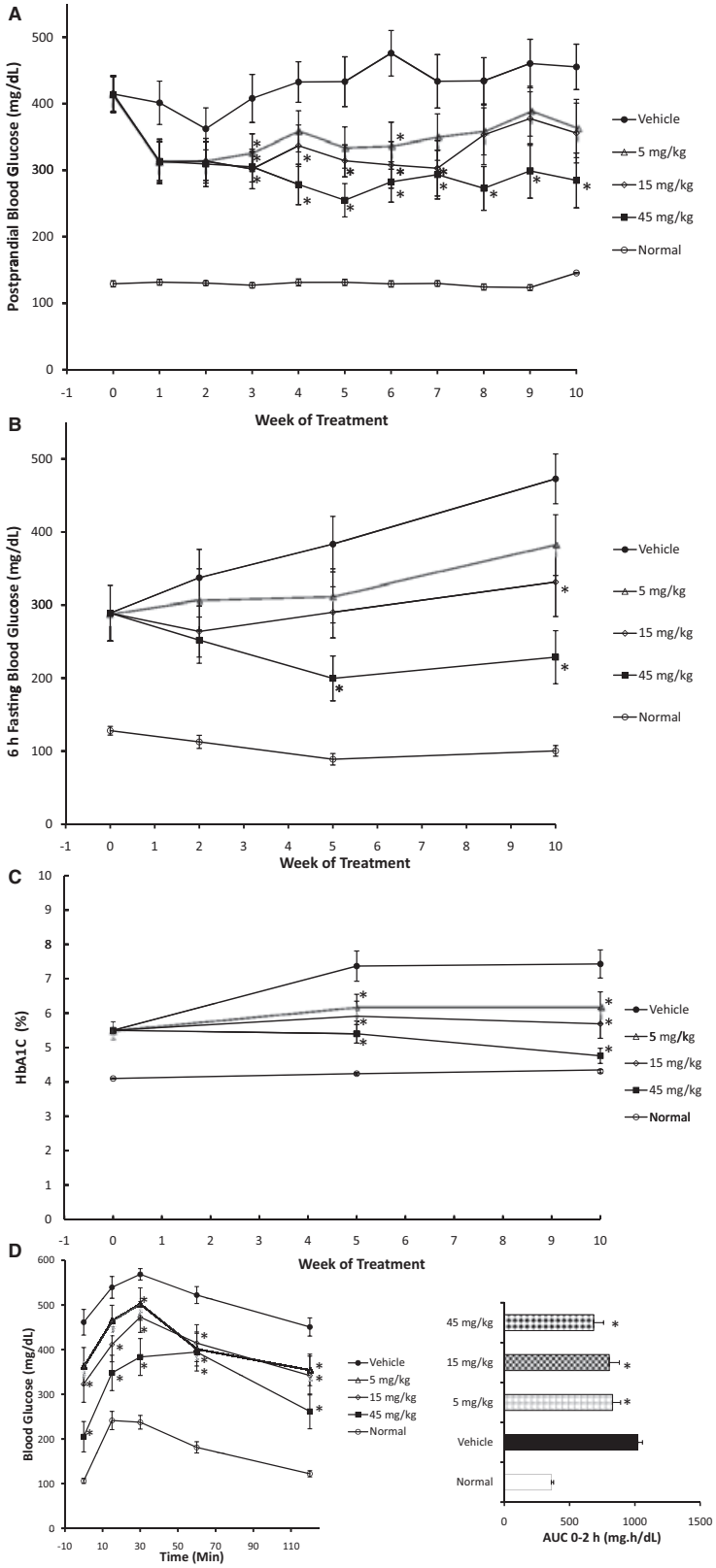

Figure 1. Effects of chronic alogliptin treatment on glycaemic control in high fat diet/streptozotocin mice. Diabetic mice were treated with alogliptin for 10 weeks by oral gavage every day at 5, 15 and 45 mg/kg, for low dose, medium dose and high dose group, respectively. The normal and vehicle group received vehicle only. Postprandial blood glucose levels (A), 6-h fasting blood glucose levels (B), A1C levels (C) and oral glucose tolerance test after 4-h fasting and the glucose area under the curve (D) were measured at the indicated time during the treatment period. Values are means ± standard error ($n = 16$ mice in each group). *$p < 0.05$ versus the vehicle-treated group.

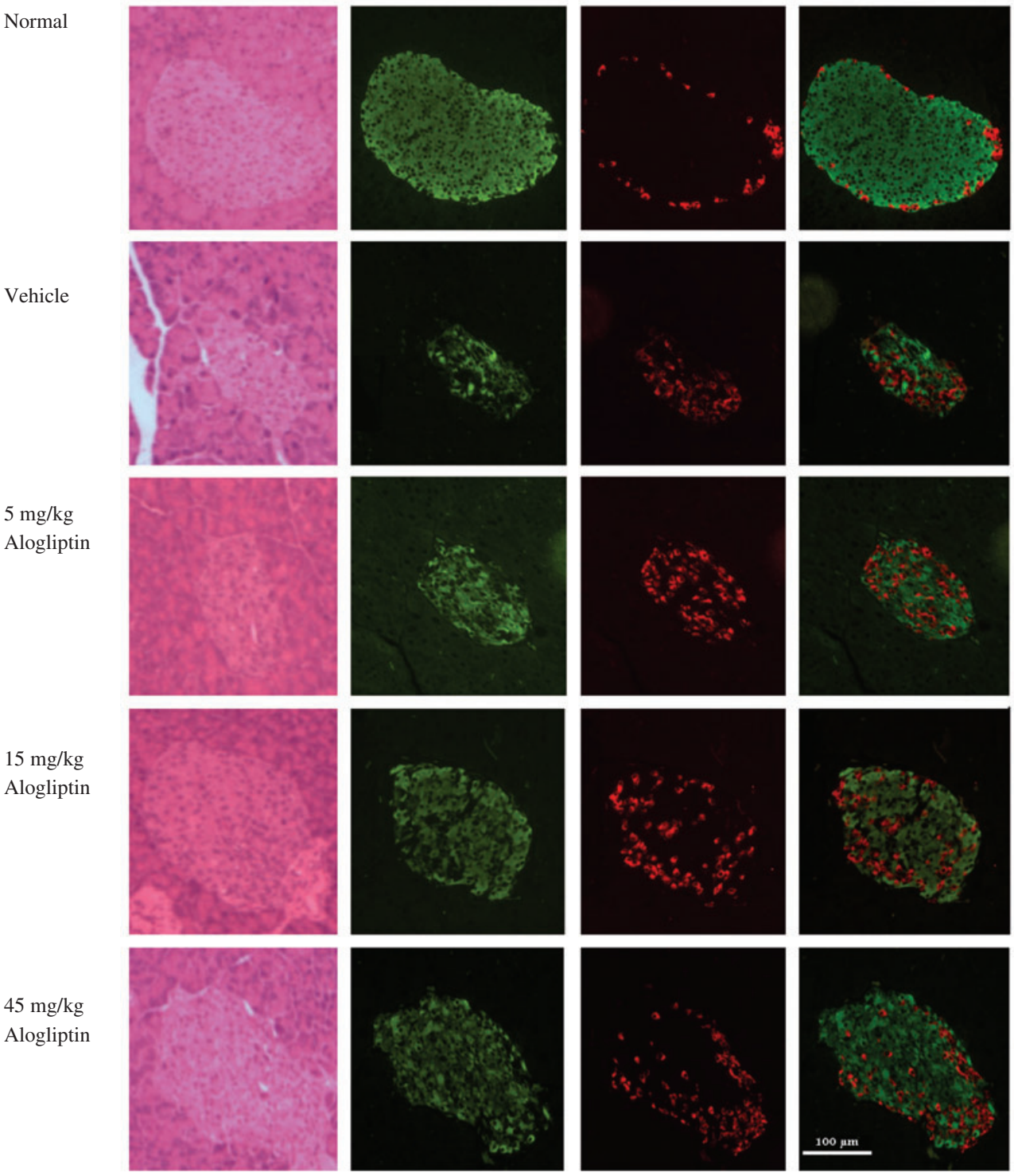

Figure 2. Histological analysis of pancreas from normal non-diabetic mice, vehicle-treated high fat diet/streptozotocin diabetic mice and alogliptin-treated diabetic mice. Pancreas sections were stained with haematoxylin and eosin or labelled with anti-insulin antibody (green) or antiglucagon antibody (red). Representative islets from each group with each staining and the overlay of the insulin and glucagon staining are shown.

and high dose, respectively). *Icam1*, *Aqp2*, *Foxp3* and *Ucp2* in diabetic mice were upregulated by 1.97-, 2.88-, 2.47- and 3.27-fold, respectively. Their expression levels were decreased but not entirely recovered to normal levels following alogliptin treatment. In addition, the recovery was not in a dose-dependent manner. Expression changes of these genes in all three treatment groups were reduced, whereas statistical significance between the normal group and alogliptin-treated

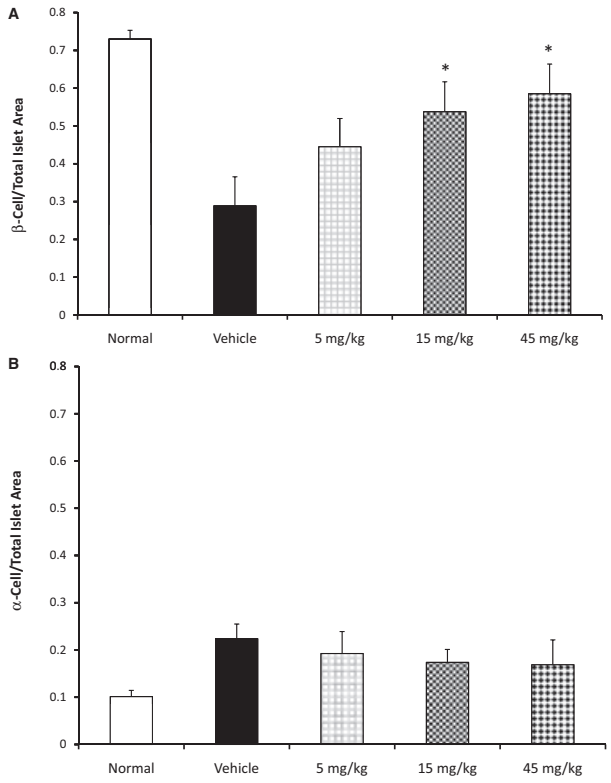

Figure 3. Morphometric analysis of islet cell composition. Images represented in figure 2 were analysed to quantify the ratio of insulin-positive β-cell mass to total islet area (A) and glucagon-positive α-cell mass to total islet area (B). The ratio was calculated from 80 islets of each group of eight mice. $^{*}p < 0.05$ versus the vehicle-treated group.

group was observed for *Icam1* in the medium dose group (FC > 1.5 and $p < 0.05$) and *Ucp2* in the high dose group (FC > 1.5 and $p < 0.05$).

The expression of *G6pc* in diabetic mice was significantly decreased (FC = −3.26). After alogliptin treatment, its expression level was back to normal range in all three dose groups. Similarly, *Neurod1* gene in diabetic mice was downgraded by 2.85-fold in comparison with that of the normal mice. Its expression was back to normal level by medium or high dose alogliptin treatment. The expression of *Ins1* was the most significantly downregulated in the vehicle group in comparison with the normal group with a reduction of almost 15 times. *Ins1* gene expression was reversed dose dependently towards the normal level by the treatment of alogliptin (Table 1).

Discussion

T2DM is an endocrine disorder involving insulin resistance and progressive pancreas functional failure. When the body develops insulin resistance, the underlying mechanism of which is still not clear, β-cell mass expands and insulin synthesis and secretion increase to compensate additional insulin demand for regulating elevated glucose level. However, overexpression of insulin and the following cellular metabolic pressure increase endoplasmic reticulum (ER) burden and intracellular reactive oxygen species production, thus impairing β-cell viability [32]. In the ensuing years, the balance between apoptosis and regeneration of β-cells is irreversibly broken and normal architecture and function of pancreas islet is gradually lost. The HFD/STZ T2DM mouse model mirrors the pathology of insulin resistance in diabetes patients, as insulin resistance occurs in most obese individuals [26–29]. In this non-genetic T2DM rodent model, β-cell mass loss and/or dysfunction by STZ insult are potentiated by peripheral insulin resistance or inflammation response induced by HFD. Ironically, while the remaining β-cells after STZ administration have to increase insulin output to normalize elevated glucose levels, this enhanced β-cell activity would bring a double-jeopardy to β-cells themselves, because of subsequent apoptosis and/or necrosis following elevated ER burden of insulin overexpression and intracellular metabolism pressure [3]. This T2DM model presented a comparable aetiology similar to human T2DM initiation and development, with partial deficiency in insulin secretion, peripheral insulin resistance and in consequence, hyperglycaemia [26–29].

In this study, chronic oral treatment of alogliptin improved glucose control and β-cell protection in HFD/STZ mice. Following alogliptin treatment for 1–2 weeks, both postprandial and 6-h fasting glucose levels were decreased in a dose-dependent manner. This results most probably from the increased plasma incretin concentrations through DPP-4 inhibition by alogliptin, as previously shown in *ob/ob* diabetic mice [25]. In addition, significant reduction of blood A1C levels in all alogliptin treatment groups provided a confirmation of improvement of overall glucose control. As GLP-1 and GIP from the gastrointestinal tract link nutrient absorption and insulin secretion from β-cells [11], partial recovery of abnormal glucose clearance after alogliptin treatment indicates an offset of impaired incretin response and β-cell functional preservation [33]. Consistent with the improved glucose control after alogliptin treatment, the β-cell mass to total islet area and islet morphology were also significantly restored, as well as pancreas insulin content and pancreas islet insulin secretion capability.

To identify the molecular mechanisms of glucose control improvement and β-cell protection by alogliptin, we analysed the changes in pancreatic gene expression. A quantitative RT-PCR analysis was performed using a mouse diabetes RT^2 profile PCR array which contains 84 diabetes-related genes. To our knowledge, this is the first study on the effects of DPP-4 inhibitors on pancreatic gene expression. Our results show that the expression of 10 genes was significantly changed in HFD/STZ diabetic mice compared with normal mice. Many of these genes are highly correlated with elevated glucose level (*Pfkfb3, Ucp2, Tgfb1, Neurod1* and *Agt*) and impaired incretin response (*G6pc*) [34–39]. Several genes' function involves important pathological processes including islet oxidative pressure (*Pfkfb3* and *Ucp2*) [40,41] and integrity of islet morphology and the extracellular matrix (*Tgfb1, Neurod1* and *Agt*) [42,43]. In addition, three genes were reported to play a role in inflammation response in pancreas tissues (*Icam1, Fpxp3* and *Agt*) [44–46].

β-Cell dysfunction and progressive β-cell mass loss represent the centrality of pathogenesis of T2DM [47]. In response

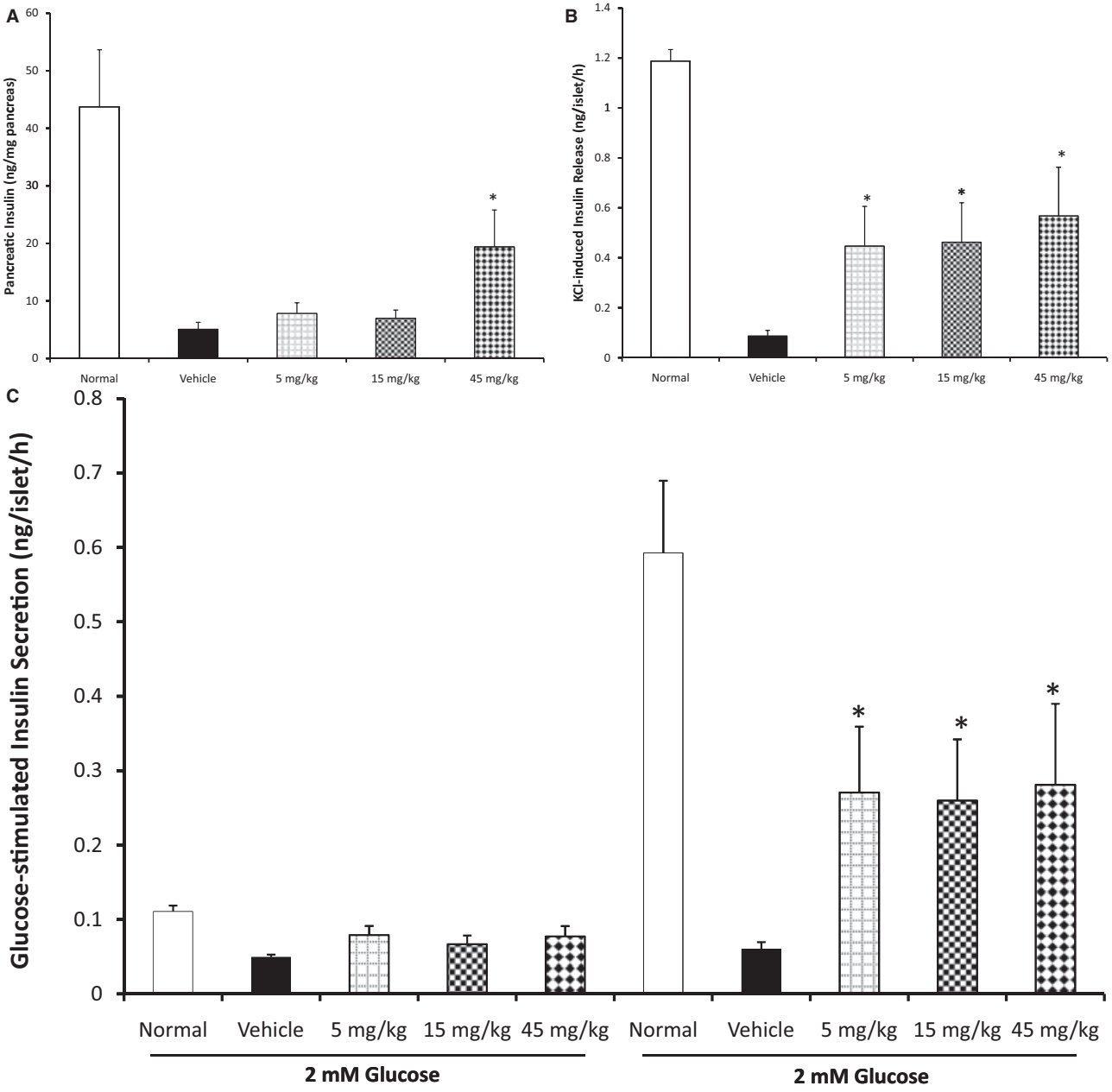

Figure 4. Alogliptin treatment increased pancreas insulin content (A), KCl-induced maximum insulin secretion (B) and increased islet glucose-stimulated insulin secretion (C). Pancreas islets were isolated from normal non-diabetic mice, vehicle-treated diabetic mice and alogliptin-treated diabetic mice. Insulin contents were quantitated with an enzyme-linked immunosorbent assay method. Insulin secretory responses to 30 mM KCl and increasing concentration of glucose were determined by a 60-min static incubation in RPMI-1640. Data are represented as means ± standard error of five islets from individual mouse. *$p < 0.05$ versus the vehicle group ($n = 8$ animals in each group).

to high glucose level and extra insulin secretion demand, upregulation of *Pfkfb3* gene indicates an accelerated glycolysis and augmentation of mitochondrial oxidative pressure [34]. The increased oxidative pressure can trigger β-cell apoptosis as these cells have a low level of antioxidant enzymes. However, the β-cell mitochondria have a self-protective mechanism by mild uncoupling of cell metabolism and ATP production, which is controlled by increased expression of mitochondrial uncoupling protein 2 (UCP2) [41]. Alogliptin treatment reversed the pathological upregulation of *Pfkfb* and *Ucp2* genes, suggesting the prevention of excessive mitochondrial superoxide production and recovery of normal β-cell intracellular metabolism. This is consistent with the result of improved GSIS and insulin maximum secretion. *Tgfb1*, *Neurod1* and *Aqp2* expression changes in diabetic mice indicate abnormal interaction between the islet and the extracellular

Table 1. The differentially expressed genes from the comparison of different groups.

		Vehicle versus normal		Low versus normal		Medium versus normal		High versus normal	
Gene	Protein description	FC	p	FC	p	FC	p	FC	p
Receptors, transporters or channels									
Icam1	Intercellular adhesion molecule 1 or CD54	1.97	0.000	1.41	0.033	1.56	0.028	1.41	0.177
Aqp2	Aquaporin 2	2.88	0.012	1.46	0.169	1.12	0.531	1.60	0.167
Transcription factors									
Foxp3	Forkhead box P3	2.47	0.023	1.22	0.972	1.30	0.844	1.72	0.269
Neurod1	Neurod1	−2.85	0.002	−1.72	0.880	−1.05	0.303	1.17	0.189
Metabolic enzymes									
Pfkfb3	6-Phosphofructo-2-kinase/fructose-2,6-biphosphatase 3	1.73	0.013	1.04	0.655	1.25	0.288	1.11	0.493
G6pc	6-Phosphofructo-2-kinase	−3.26	0.049	1.02	0.823	−1.24	0.354	1.26	0.856
Secreted factors									
Agt	Angiotensinogen	1.93	0.013	1.50	0.099	1.37	0.254	1.20	0.383
Ins1	Insulin I	−14.69	0.001	−4.69	0.574	−2.75	0.298	−1.91	0.976
Tgfb1	Transforming growth factor, β1	1.59	0.031	1.01	0.908	1.03	0.831	1.05	0.818
Mitochondrial anion carrier proteins									
Ucp2	Mitochondrial uncoupling protein 2	3.27	0.003	1.38	0.243	1.57	0.133	2.10	0.024

FC, fold change.

matrix and deficiency in islet morphology remodelling. As a member of the transforming growth factor β family and encoded by *Tgfb1*, TGFβ1 medicates glucose homeostasis in the extracellular matrix and regulates β-cell function and proliferation [42]. NeuroD1, encoded by *Neurod1*, is a key transcription factor required for islet morphogenesis to form properly organized sphere-like structures [37]. Aquaporin 2, the gene product of *Aqp2*, helps keeping water homeostasis and maintains cellular osmolality in response to osmolality changes in the blood. The recovery of expression of these genes following alogliptin treatment suggests the revival of β-cells and islets, which corresponds to the normalization of β-cell morphology and islet architectural remodelling shown in the immunohistochemistry analysis.

Icam 1, *Foxp3* and *Agt* gene expressions are related to inflammation and immune response. Upregulation of *Icam1* gene expression in diabetic pancreas implies an elevation of monocyte recruitment and monocyte differentiation into macrophage, which indicates an increased inflammation response [4]. On the other hand, upregulated expression of *Foxp3* gene suggests an enhanced inhibition of T-cell differentiation and autoimmunity [45]. Therefore, our results are consistent with the common understanding that β-cell death in T2DM is mostly because of necrosis and dead cells are cleared by macrophages. Upregulation of *Agt* gene expression, which encodes angiotensinogen—one of the major components in rennin–angiotensin system–indicates elevated oxidative stress and inflammation response [46]. Chronic treatment of alogliptin reduced the expression of all these three genes, suggesting an alleviated inflammation response.

Last but not the least, with all the gene expression changes and their negative effects on islet structure and function mentioned above, it was not surprising to find out that *Ins1* expression was significantly reduced in diabetic mice, consistent with the significant decrease of pancreatic insulin content found in this study. After alogliptin treatment, it was observed that insulin gene expression was recovered significantly, along with an improved glucose control. Although the gene expression study reveals some of the key mechanisms for diabetic development and alogliptin mechanisms of action, a genome-wide gene expression profiling analysis on the same tissue samples is needed for gaining the complete understanding of the underlying mechanisms. In addition, functional genomic studies are needed to validate the roles in the course of diabetic pathogenesis of these genes identified in this study.

In summary, chronic administration of alogliptin in HFD/STZ mice improved glucose control and islet structure and function. Pancreatic gene expression profiles provide important information for understanding the possible molecular mechanisms for alogliptin's action, which may involve alleviating ER and oxidation stress, increasing β-cell differentiation and proliferation and remodelling islet architecture and preserving its function. Our results support the clinical trial results that alogliptin is a promise agent for T2DM therapy with disease-modifying properties.

Acknowledgement

The authors were supported by Takeda Pharmaceuticals North America.

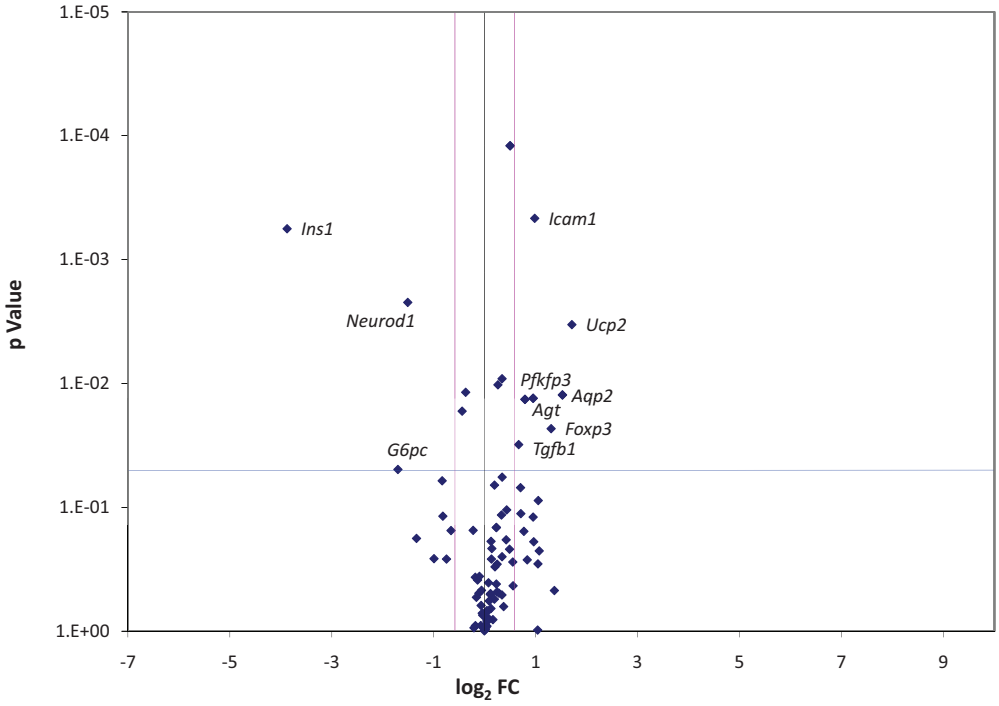

Figure 5. Volcano plot of gene expression data from mice pancreas in vehicle group and normal group. The *x*-axis is the differences in log 2 expression value between vehicle group and normal group, whereas the statistical significance between treated and control groups is shown in the *y*-axis. Each dot in the figure represents a gene presented in the PCR array. Genes shown in the upper-right corner and the upper-left corner are significantly upregulated and downregulated genes, respectively, under a combination of selection criteria of fold change (FC) > 1.5 and $p < 0.05$. The blue line indicates the desired threshold for the p value (0.05) of the *t*-test, whereas the pink line indicates the FC > 1.5 or <-1.5. n = 8 mice in each group.

Conflict of Interest

X. Z., Y. H. and J. W. helped in the design of this study. X. Z., Z. W. and J. W. helped in the conduct/data collection and analysis of the manuscript. X. Z., Z. W., Y. H. and J. W. helped in writing the manuscript. All the authors have no competing interests.

Supporting Information

Additional Supporting Information may be found in the online version of this article:

Table S1. The differentially expressed genes from the comparison of different groups (FC, fold change) of all the 84 diabetes-related genes (including the internal control genes).

Please note: Wiley-Blackwell are not responsible for the content or functionality of any supporting materials supplied by the authors. Any queries (other than missing material) should be directed to the corresponding author for the article.

References

1. Perley MJ, Kipnis DM. Plasma insulin responses to oral and intravenous glucose: studies in normal and diabetic subjects. J Clin Invest 1967; **46**: 1954–1962.
2. Bonora E. Protection of pancreatic beta-cells: is it feasible? Nutr Metab Cardiovasc Dis 2008; **18**: 74–83.
3. Wajchenberg BL. β-Cell failure in diabetes and preservation by clinical treatment. Endocr Rev 2007; **28**: 187–218.
4. Shoelson SE, Lee J, Goldfine AB. Inflammation and insulin resistance. J Clin Invest 2006; **116**: 1793–1801.
5. Bajaj M, Defronzo RA. Metabolic and molecular basis of insulin resistance. J Nucl Cardiol 2003; **10**: 311–323.
6. Schinner S, Scherbaum WA, Bornstein SR, Barthel A. Molecular mechanisms of insulin resistance. Diabet Med 2005; **22**: 674–682.
7. Panunti B, Jawa AA, Fonseca VA. Mechanisms and therapeutic targets in type 2 diabetes mellitus. Drug Discov Today Dis Mech 2004; **2**: 151–157.
8. Wild S, Roglic G, Green A, Sicree R, King H. Global prevalence of diabetes: estimates for the year 2000 and projections for 2030. Diabetes Care 2004; **27**: 1047–1053.
9. Cohen A, Horton ES. Progress in the treatment of type 2 diabetes: new pharmacologic approaches to improve glycemic control. Curr Med Res Opin 2007; **23**: 905–917.
10. Verspohl EJ. Novel therapeutics for type 2 diabetes: incretin hormone mimetics (glucagon-like peptide-1 receptor agonists) and dipeptidyl peptidase-4 inhibitors. Pharmacol Ther 2009; **124**: 113–138.
11. Baggio LL, Drucker DJ. Biology of incretins: GLP-1 and GIP. Gastroenterology 2007; **132**: 2131–2157.
12. Xu G, Stoffers DA, Habener JF, Bonner-Weir S. Exendin-4 stimulates both beta-cell replication and neogenesis, resulting in increased beta-cell mass and improved glucose tolerance in diabetic rats. Diabetes 1999; **48**: 2270–2276.
13. Fan R, Li X, Gu X, Chan JC, Xu G. Exendin-4 protects pancreatic beta cells from human islet amyloid polypeptide-induced cell damage: potential

involvement of AKT and mitochondria biogenesis. Diabetes Obes Metab 2010; **12**: 815–824.

14. Salehi M, Aulinger BA, D'Alessio DA. Targeting beta-cell mass in type 2 diabetes: promise and limitations of new drugs based on incretins. Endocr Rev 2008; **29**: 367–379.
15. Combettes MM. GLP-1 and type 2 diabetes: physiology and new clinical advances. Curr Opin Pharmacol 2006; **6**: 598–605.
16. Siddiqui NI. Incretin mimetics and DPP-4 inhibitors: new approach to treatment of type 2 diabetes mellitus. Mymensingh Med J 2009; **18**: 113–124.
17. Lambeir AM, Durinx C, Scharpé S, De Meester I. Dipeptidyl-peptidase IV from bench to bedside: an update on structural properties, functions, and clinical aspects of the enzyme DPP IV. Crit Rev Clin Lab Sci 2003; **40**: 209–294.
18. Nauck M, Stöckmann F, Ebert R, Creutzfeldt W. Reduced incretin effect in type 2 (non-insulin-dependent) diabetes. Diabetologia 1986; **29**: 46–52.
19. Zarowitz BJ, Conner C. The intersection of safety and adherence: new incretin-based therapies in patients with type 2 diabetes mellitus. Pharmacotherapy 2009; **29**: 55S–67S.
20. Feng J, Zhang Z, Wallace MB et al. Discovery of alogliptin: a potent, selective, bioavailable, and efficacious inhibitor of dipeptidyl peptidase IV. J Med Chem 2007; **50**: 2297–2300.
21. Lee B, Shi L, Kassel DB, Asakawa T, Takeuchi K, Christopher RJ. Pharmacokinetic, pharmacodynamic, and efficacy profiles of alogliptin, a novel inhibitor of dipeptidyl peptidase-4, in rats, dogs, and monkeys. Eur J Pharmacol 2008; **589**: 306–314.
22. Ikeda H, Shino A, Matsuo T, Iwatsuka H, Suzuoki Z. A new genetically obese-hyperglycemic rat (Wistar fatty). Diabetes 1981; **30**: 1045–1050.
23. Matsuo T, Odaka H, Ikeda H. Effects of an intestinal disaccharidase inhibitor (AO-128) on NIDDM and IDDM rat models. In: Goto Y, Kanazawa Y eds. Lessons from Animal Diabetes. The Tokyo Workshop 1990. London: Smith-Gordon; 171–175.
24. Takeuchi K, Moritoh Y, Asakawa T et al. Effects of SYR-322, a novel inhibitor of dipeptidyl peptidase-IV alone or in combination with pioglitazone in obese and non-obese type 2 diabetes model rats and mice. Diabetes 2006; **55**: A465.
25. Moritoh Y, Takeuchi K, Asakawa T, Kataoka O, Odaka H. Chronic administration of alogliptin, a novel, potent, and highly selective dipeptidyl peptidase-4 inhibitor, improves glycemic control and beta-cell function in obese diabetic ob/ob mice. Eur J Pharmacol 2008; **588**: 325–332.
26. Luo J, Quan J, Tsai J et al. Nongenetic mouse models of non-insulin-dependent diabetes mellitus. Metabolism 1998; **47**: 663–668.
27. DeFronzo RA. Pharmacologic therapy for type 2 diabetes mellitus. Ann Intern Med 1999; **131**: 281–303.
28. Mu J, Woods J, Zhou YP et al. Chronic inhibition of dipeptidyl peptidase-4 with a sitagliptin analog preserves pancreatic beta-cell mass and function in a rodent model of type 2 diabetes. Diabetes 2006; **55**: 1695–1704.
29. Mu J, Petrov A, Eiermann GJ et al. Inhibition of DPP-4 with sitagliptin improves glycemic control and restores islet cell mass and function in a rodent model of type 2 diabetes. Eur J Pharmacol 2009; **623**: 148–54.
30. Lacy PE, Kostianovsky M. Method for the isolation of intact islets of Langerhans from the rat pancreas. Diabetes 1967; **16**: 35–39.
31. Korbutt GS, Elliott JF, Ao Z, Smith DK, Warnock GL, Rajotte RV. Large scale isolation, growth, and function of porcine neonatal islet cells. J Clin Invest 1996; **97**: 2119–2129.
32. McCabe C, Samali A, O'brien T. β cell cytoprotective strategies: establishing the relative roles for iNOS and ROS. Biochem Biophys Res Commun 2006; **342**: 1240–1248.
33. Toft-Nielsen MB, Damholt MB, Madsbad S et al. Determinants of the impaired secretion of glucagon-like peptide-1 in type 2 diabetic patients. J Clin Endocrinol Metab 2001; **86**: 3717–3723.
34. Yaney GC, Schultz V, Cunningham BA, Dunaway GA, Corkey BE, Tornheim K. Phosphofructokinase isozymes in pancreatic islets and clonal β-cells (INS-l). Diabetes 1995; **44**: 1285–1289.
35. Yamashita T, Eto K, Okazaki Y et al. Role of uncoupling protein-2 up-regulation and triglyceride accumulation in impaired glucose-stimulated insulin secretion in a β-cell lipotoxicity model overexpressing sterol regulatory element-binding protein-1c. Endocrinology 2004; **145**: 3566–3577.
36. McGinn S, Poronnik P, King M, Gallery ED, Pollock CA. High glucose and endothelial cell growth: novel effects independent of autocrine TGF-β1 and hyperosmolarity. Am J Physiol Cell Physiol 2003; **284**: 1374–1386.
37. Naya FJ, Huang HP, Qiu Y et al. Diabetes, defective pancreatic morphogenesis, and abnormal enteroendocrine differentiation in BETA2/NeuroD-deficient mice. Genes Dev 1997; **11**: 2323–2334.
38. Mobasheri A, Wray S, Marples D. Distribution of AQP2 and AQP3 water channels in human tissue microarrays. J Mol Histol 2005; **36**: 1–14.
39. Dachicourt N, Serradas P, Giroix MH, Gangnerau MN, Portha B. Decreased glucose-induced cAMP and insulin release in islets of diabetic rats: reversal by IBMX, glucagon, GIP. Am J Physiol 1996; **271**: E725–E732.
40. Roche E, Assimacopoulos-Jeannet F, Witters LA et al. Induction by glucose of genes coding for glycolytic enzymes in a pancreatic β-cell line (INS-1). J Biol Chem 1997; **272**: 3091–3098.
41. Vidal-Puig AJ. Uncoupling expectations. Nat Genet 2000; **26**: 387–388.
42. Brown ML, Schneyer AL. Emerging roles for the TGF β family in pancreatic β-cell homeostasis. Trends Endocrinol Metab 2010; **21**: 441–448.
43. Itkin-Ansari P, Marcora E, Geron I et al. NeuroD1 in the endocrine pancreas: localization and dual function as an activator and repressor. Dev Dyn 2005; **233**: 946–953.
44. Kim I, Moon SO, Kim SH, Kim HJ, Koh YS, Koh GS. Vascular endothelial growth factor expression of intercellular adhesion molecule 1 (ICAM-1), vascular cell adhesion molecule 1 (VCAM-1), and E-selectin through nuclear factor-κB Activation in endothelial cells. J Biol Chem 2001; **276**: 7614–7620.
45. Korn T, Anderson AC, Bettelli E, Oukka M. The dynamics of effector T cells and Foxp3+ regulatory T cells in the promotion and regulation of autoimmune encephalomyelitis. J Neuroimmunol 2007; **191**: 51–60.
46. Leung PS, Carlsson PO. Tissue renin-angiotensin system: its expression, localization, regulation and potential role in the pancreas. J Mol Endocrinol 2001; **26**: 155–164.
47. Gautier JF, Fetita S, Sobngwi E, Salaün-Martin C. Biological actions of the incretins GIP and GLP-1 and therapeutic perspectives in patients with type 2 diabetes. Diabetes Metab 2005; **31**: 233–242.